Scalar Field Dark Matter and Nucleosynthesis

Preliminary Examination Report

James Wheeler

June 13, 2020

Abstract

Fuzzy (or wave) dark matter is a family of dark matter models characterized by a dynamical matter field satisfying a wave equation, most typically a scalar field (real or complex) satisfying the Klein-Gordon equation with a mass (or frequency) parameter $m \approx 10^{-20 \pm 4}$ eV $\approx 10^{2 \pm 4}$ years^{-1}. While it is well-known that such a scalar field has the potential to dominate the early universe's energy density due to a phase transition in which its energy switches from scaling as a^{-3} at late times ($H << m$) to a^{-6} at early times ($H >> m$), the cosmological implications of this dominance have not been thoroughly explored, presumably due to motivations within popular models (such as ultralight axion-like particles) for choosing initial conditions that suppress the a^{-6} behavior. Without such motivations, these initial conditions would appear rather fine-tuned. Recognizing the existence of alternative models for scalar field FDM (such as a scalar field arising due to a nontrivial connection) that do not favor these suppressing initial conditions, then, it is necessary to consider the full range of cosmological behavior supported by these models. It is my objective to explore these behaviors, specifically as they relate to cosmology's remarkably accurate predictions of light element abundances through big bang nucleosynthesis (BBN). While preliminary results suggest that scalar field FDM is not able to resolve the so-called Lithium problem of BBN, it seems that a combination of stability and BBN considerations can constrain the mass parameter in the case of a complex scalar field to $m \gtrsim 10^{-20}$ eV.

1 Introduction

General Relativity (GR) has proven a remarkably powerful tool in enhancing our understand of the universe on length scales of and beyond our solar system, from its corrections to the orbit of mercury and gravitational lensing to the standard model of cosmology, known as ΛCDM. Perhaps the largest outstanding critical problem for general relativity, however, is that of identifying of the nature of dark matter. The concept of dark matter is an answer to the puzzling observed phenomenon that, supposing gravity behaves according to general relativity (or, on smaller scales, Newtonian gravitation), various astronomical systems behave as if there is much more mass present, interacting gravitationally with visible matter, than we can see.

This phenomenon has been on the minds of physicists for more than a century: based on his measurements of the velocity dispersion of stars in the Milky Way galaxy, Lord Kelvin explicitly posited as early as 1904 that "many of our stars, perhaps a great majority of them, may be dark bodies" [10]. It wasn't until several decades later, however, that this hypothesis began to be taken seriously by astronomers, as measurements of both velocity dispersions of galaxies within clusters and the flatness of galaxy rotation curves suggested similar conclusions (Figure 1).

Though the need for a theoretical explanation for this behavior was more or less experimentally well-established by the 1970's, it remained unclear what the most appropriate answer might be, a situation that has persisted to the current day. Explanatory hypotheses abound and can be broadly categorized as either suggesting the nature of unseen matter or modifying the theory of gravity so that the visible matter is sufficient to yield the observed behavior under the modified theory. Perhaps the most popular among theories modifying gravity is the theory of Modified Newtonian Dynamics (MOND), which phenomenologically alters the law of Newtonian Gravitation at sufficiently small accelerations. Such models are often criticized as appearing ad hoc, but the astrophysical community's larger objection to modified gravity theories stems from the 2006 analysis [6] of the so-called bullet cluster (Figure 2), a pair of recently-collided galaxy clusters for which lensing data suggests that the apparently missing mass separated considerably from the visible matter in the course of the collision. Generally speaking, one might expect that the most simply implemented theories of modified gravity would predict that the apparently missing mass closely tracks the visible matter. As this analysis demonstrates such tracking doesn't always happen in
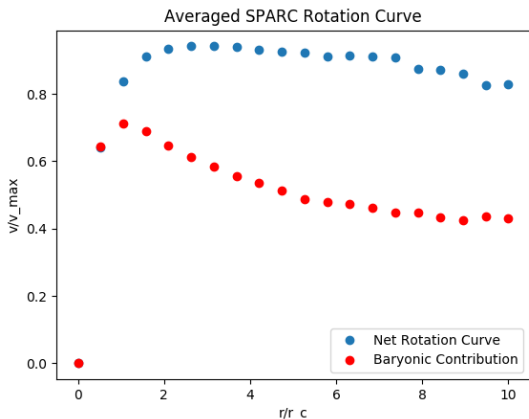
Figure 1: An average scaled-axes rotation curve created from the SPARC database of measurements of rotational velocities within 175 galaxies [12]. Blue points trace the measured rotational velocities, while red points trace the rotational velocities expected based upon the amount of visible matter. The discrepancy between these data sets indicates the need for missing matter providing the addition radial acceleration, and that this behavior is consist across galaxies. Averaging process and image creation by Ben Hamm.
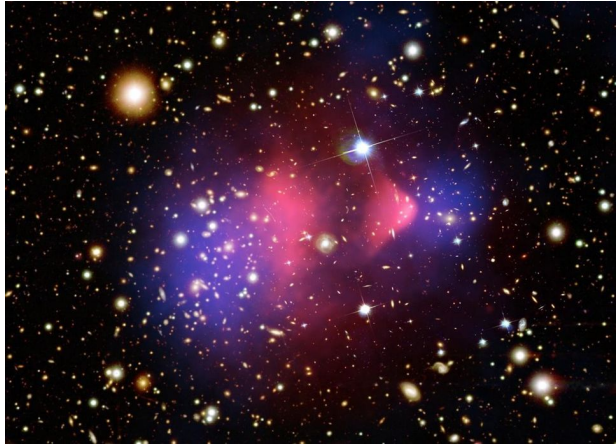

Figure 2: An image illustrating the 2006 analysis of the bullet cluster. The pink overlay is in the x-ray spectrum, indicating the location of the bullet cluster's visible matter, while the blue overlay is the mass distribution computed via gravitational lensing. Image created by the Chandra X-ray Center (visible matter) and the Space Telescope Science Institute (optical image and lensing map).

reality, it is seen by many as sufficient reason to focus attention on theories of unseen, or dark, matter.

What observational constraints can be put on dark matter? Perhaps the most significant cosmological constraint is that (a nontrivial component of) dark matter must be cold for most of the universe's history. This means that dark matter's cosmological pressure is negligible compared to its energy density, as for a gas in thermal equilibrium at a temperature much smaller than the particle mass (hence the denomination "cold"). The observational data demanding this feature are galaxy sizes and the extent to which the Cosmic Microwave Background (CMB) temperature is isotropic, both of which are quite well-established. Following the gas analogy, which is not an analogy at all in particle models of dark matter, negligible pressure corresponds to gas particles moving nonrelativistically, and so the heuristic explanation of the cold constraint is that, given seed perturbations of dark matter at scales set by the variation in the CMB, particles moving too quickly (that are too "hot") cannot be bound gravitationally on scales as small as galaxies.

The prevailing model of cold dark matter, built into the remarkably successful ΛCDM standard model of cosmology, is that of a Weakly Interacting Massive Particle (WIMP) sufficiently heavy to be cold. This model does very well cosmologically, but has some shortcomings on the scale of galaxies, in particular the cusp-core problem: many-body simulations of in-

teracting WIMP clusters consistently develop sharp, cuspy density profiles at the centers of galaxies, a phenomenon not observed in actual galaxies, which tend to have smooth cores of density at their centers. Other issues for the WIMP model include the missing satellites problem, a discrepancy between the number of observed and predicted persisting satellite galaxies orbiting a host, and the too-big-to-fail problem, a prediction by WIMP simulations of dark matter subhalos with higher central densities than observed in Milky Way satellites. While there may be potential to resolve these issues by incorporating more sophisticated baryonic physics, as investigated in [11] and [15], they (together with the fact that searches for WIMP candidates have so far turned up null) are sufficient motivation to explore alternative models.

A family of models that can serve as potential alternatives to the WIMP model is Fuzzy (or wave) dark matter, often abbreviated FDM or ψDM, within which models are characterized by a dynamical matter field satisfying a wave equation. The simplest example among this family of models is that of a scalar field (real or complex) satisfying the Klein-Gordon equation with a mass (or frequency) parameter $m \approx 10^{-20\pm4}$ eV $\approx 10^{2\pm4}$ years^{-1}. More explicitly, on the spacetime manifold (M, g) there is a function $\psi : M \to \mathbb{C}$ with associated stress energy tensor and constraint equation

$$T = \frac{d\psi \otimes d\bar{\psi} + d\bar{\psi} \otimes d\psi}{m^2} - \left(\frac{|d\psi|^2}{m^2} + |\psi|^2 \right) g \quad (1)$$

$$\Box\psi = m^2\psi. \quad (2)$$

This simplest example, referred to as Scalar Field Dark Matter (SFDM), demonstrates promise in that it can replicate many of the cosmological successes of the WIMP model–the heuristic reason one might expect this is that the frequency parameter sets a characteristic length scale $\frac{2\pi}{m} \approx 10^{-1\pm4}$ lyr of wave packets, far above which the dynamics should be similar to that of many gravitationally interacting particles–while simultaneously resolving some of the galaxy-scale concerns listed above in a natural way [8], especially that of the cusp-core problem.

What might this scalar field ψ be describing? Perhaps the most popular motivation for considering SFDM is that it is an approximate description for ultralight axion-like particles (in regimes where self interaction terms can be neglected), predicted within some contexts of string theory [21]. Importantly, this motivation for considering SFDM leads to natural choices for dark matter's initial velocity and power spectrum when modifying ΛCDM cosmology. However, this is not the only motivation for SFDM.

Standard general relativity is obtained by extremizing the Einstein-Hilbert action, which has long been known to be the most general admissible action quadratic in the metric coefficients g_{ij} and their coordinate derivatives [13]. In [5], Hubert Bray found that slightly generalizing the action to also be quadratic in the connection coefficients $\Gamma_{ij}{}^k$ and their coordinate derivatives generically leads to a modification of GR wherein the tensor T of equation (1), for some real-valued function ψ parameterizing the connection's deviation from the Levi-Civita connection of standard GR, is added to the stress energy tensor of matter in Einstein's equation. That is, this mild generalization of the action of GR naturally leads to a model of SFDM, wherein the additional "matter" is, in fact, an artifact of a nontrivial connection. Clearly, such a model leads to a different quantum interpretation of ψ for which the natural choices of initial velocity and power spectrum referenced above are lost. In light of this alternative motivation for SFDM, my primary research objective is currently to identify cosmological variations that SFDM allows for when one does not restrict to the standard initial conditions.

2 SFDM Cosmology and BBN

2.1 SFDM in Basic Cosmology

At the foundation of cosmology is the homogeneous and isotropic universe, modeled via the spacetime manifold $(\mathbb{R}_+ \times \Sigma, g)$ together with a homogeneous Riemannian metric h on the 3-manifold Σ satisfying $g = -dt^2 + a(t)^2 h$. In light of observational constraints on the magnitude of the (constant) sectional curvature of h [1], we will restrict to the case that h is flat, requiring that (Σ, h) be a quotient of $\mathbb{R}^3$; in terms of natural (x_1, x_2, x_3) coordinates on $\mathbb{R}^3$, we then have

$$g = -dt^2 + a(t)^2(dx_1^2 + dx_2^2 + dx_3^2). \qquad (3)$$

Utilizing the stress energy tensor T of equation (1) for real-valued ψ (the complex case will be identical to two independent real-valued fields), we wish to solve the coupled system of Einstein's equation

$$G = 8\pi T \qquad (4)$$

and the Klein-Gordon equation (2) on the homogeneous and isotropic universe. The first step is recognizing that the isotropy of G under the ansatz (3) requires the same of T, and therefore of $d\psi \otimes d\psi$. Dualizing in the first slot, isotropy requires that the $(1,1)$-tensor $\nabla\psi \otimes d\psi$, thought of as an endomorphism of the tangent space, must restrict to a multiple of the identity operator on the spatial subspace spanned by $\{\partial_i\}_{i=1}^3$, but since the image of this map is at most one dimensional (being the span of $\nabla\psi$) this multiple must be zero– that is, we must have $0 = d\psi(\partial_i) = \partial_i\psi$, or $\psi = \psi(t)$ is a function of t only.

With this constraint, the energy density $\rho_\psi := T(\partial_t, \partial_t)$ and pressure $p_\psi := T(\partial_i, \partial_i)$ associated to ψ on the constant-time slices $\Sigma_t := \{t\} \times \Sigma$ are given by

$$\rho_\psi(t) = \frac{\dot{\psi}(t)^2}{m^2} + \psi(t)^2 \quad p_\psi(t) = \frac{\dot{\psi}(t)^2}{m^2} - \psi(t)^2. \quad (5)$$

In terms of these and the Hubble parameter $H(t) := \frac{\dot{a}(t)}{a(t)}$, equations (2) and (4) amount to

$$\ddot{\psi} + 3H\dot{\psi} + m^2\psi = 0 \qquad (6)$$

$$\dot{\rho} = -3H(\rho + p) \qquad (7)$$

$$H^2 = \frac{8\pi}{3}\rho, \qquad (8)$$

where one can now more generally interpret ρ and p as being the sums of the energy density and pressure of all types of matter– ψ, baryonic matter, radiation, and dark energy. In the simplest treatments ignoring energy transfer between the types of matter, equation (7) holds for each type of matter individually.

In the case that the source matter satisfies the equation of state $p = w\rho$ for w constant (typical cases include $w = 0$ for baryonic matter or WIMP CDM, $w = 1/3$ for radiation, and $w = -1$ for dark energy), equation (7) reads $\dot{\rho} = -3H(1 + w)\rho$, yielding
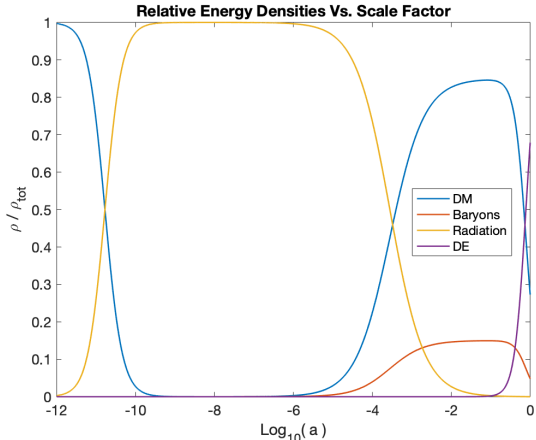
$$\rho \propto a^{-3(1+w)} \qquad (9)$$

3

Figure 3: Relative energy densities of the matter sources versus scale factor in a typical SFDM cosmology. In this cosmology, dark matter dominates the energy density once the scale factor satisfies $a \lesssim 10^{-11}$; this corresponds to $T_t \approx 10$ MeV (see section 3.1 for the definition of the transition temperature T_t).
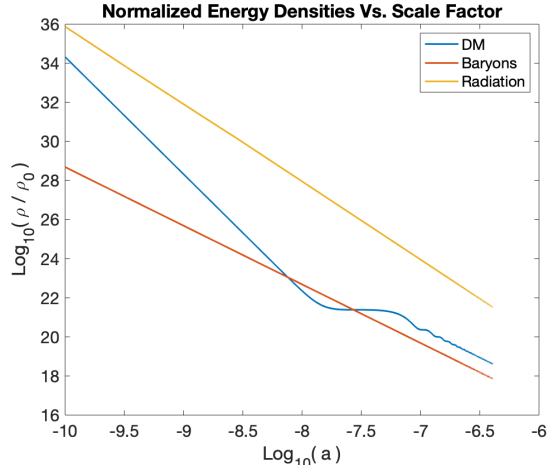

Figure 4: Energy densities of the matter sources (normalized to the current critical density) versus scale factor in the cosmology of Figure 3. The $\rho_\psi \propto a^{-6}$ era is seen to be $a \lesssim 10^{-8}$; the $\rho_\psi \approx$ constant era is roughly $10^{-7.9} \lesssim a \lesssim 10^{-7.2}$; and the $\rho_\psi \propto a^{-3}$ era is $a \gtrsim 10^{-7}$.

and, putting this into (8) for the case that this source dominates the total energy density,

$$a(t) \propto (t - t_0)^{\frac{2}{3(1+w)}}. \tag{10}$$

With this in mind, we identify three regimes of behavior for ψ. The first is $H << m$ (we will refer to this era as "late"), in which case equation (6) may be approximated as $\ddot{\psi} = -m^2\psi$, so that ψ oscillates with frequency m (with period therefore roughly in the range of days to years), leading to the observation per equation (5) that $p_\psi << \rho_\psi$ when averaged over many periods, so the energy contribution of ψ in this regime is well approximated by the $w = 0$ case (that is, ψ is cold in this regime). Solving backwards from the current time, this first regime holds until $H \approx m$, which occurs roughly at a time $t \sim 1/m$ after the singularity due to equation (10), which implies that $H \sim 1/t$. Since $t \sim 1/m$ is well before the time of matter-radiation equality, $H >> m$ begins (evolving time backward) in the radiation dominated era, wherein $w = 1/3$.

The remaining two regimes of interest occur when $H >> m$, in which case equation (6) may be approximated as $\ddot{\psi} = -3H\dot{\psi}$, so that $\dot{\psi} \propto a^{-3}$. Combining this with equation (10) while the energy density is dominated by a matter source with constant equation of state, we then have

$$\psi - \psi_0 \propto (t - t_0)^{\frac{w-1}{w+1}} \propto a^{\frac{3(w-1)}{2}} \tag{11}$$

(or $\ln(a)$ in the event $w = 1$). In particular, we begin with $w = 1/3$, so that $\psi - \psi_0 \propto a^{-1}$, with

which we can understanding the behavior of ψ for large and small a. For large a, $\dot{\psi} \to 0$ and $\psi \to \psi_0$ means ψ behaves like a contribution to dark energy (still negligible compared to radiation). For small a, $\frac{\dot{\psi}}{m}$ eventually becomes much bigger than ψ, so that $\rho_\psi \propto a^{-6}$ and this eventually overtakes the radiation density $\rho_r \propto a^{-4}$. Our two remaining regimes, then, are characterized by $\rho_\psi \propto a^{-6}$, which occurs and persists once one gets close enough to the big bang (only potentially adjusting during the inflationary era) and leads to dark matter domination in the early universe, and $\rho_\psi \approx$ constant, which occurs once $\frac{\dot{\psi}}{m}$ becomes significantly smaller than ψ and persists until $H \approx m$.

Observe that the $\rho_\psi \approx$ constant era can either not be present at all or extend back arbitrarily close to the big bang (even until the inflationary era, effectively eliminating the $\rho_\psi \propto a^{-6}$ era) depending on one's choice of initial condition for ψ and $\dot{\psi}$ (as a late-time initial condition, this amounts to a choice of phase in the oscillation) by making $\frac{\dot{\psi}}{m}$ either bigger or sufficiently smaller than ψ at $H \approx m$. The axion-like particle perspective on SFDM typically argues that axions are produced with low momentum [18], so that $\dot{\psi}$ is always small, eliminating the $\rho_\psi \propto a^{-6}$ era in favor of $\rho_\psi \approx$ constant. From the geometric perspective of SFDM, however, such a choice appears arbitrary and fine-tuned; hence, it is natural to ask what observable implications allowing the $\rho_\psi \propto a^{-6}$ era might have.

4

2.2 Big Bang Nucleosynthesis

Among the deepest and most impressive predictions of the standard ΛCDM cosmology are the light element abundances– specifically the abundances of Deuterium, ^{3}He, ^{4}He, and ^{7}Li relative to Hydrogen– some minutes after the big bang. As one travels back in time toward the Big Bang, the universe compresses, causing the ambient temperature to diverge as $a \to 0$. Early enough, then, all standard model particles are relativistic and in thermal equilibrium, forming a radiation bath. As the universe expands and the temperature drops, particle-antiparticle pairs annihilate, quarks and gluons combine into baryonic bound states, and most of the remaining massive particles become non-relativistic, leading to their number densities becoming exponentially suppressed by the Boltzmann factor $e^{-m/T}$ while they remain thermodynamically coupled to the radiation bath via electromagnetic and weak interactions.

As the universe continues to expand, however, the interactions coupling various particles and nuclides to the radiation become too slow compared to the universe's expansion, leading to their abundances "freezing out". In particular, weak interactions effectively stop at approximately $T \sim 1$ MeV (about 1 second after the Big Bang), so that the relative abundance of neutrons to protons freezes out. Around $T \sim 0.1$ MeV, these protons and neutrons begin synthesizing into deuterium in appreciable amounts, opening the floodgate for larger nuclides to be built. A large network of coupled Boltzmann equations, one for each possible nuclear reaction between the various nuclides, then determines how nuclide abundances (relative to Hydrogen) evolve over time in a process known as Big Bang Nucleosynthesis (BBN). Several minutes after the Big Bang, the rates of the involved nuclear reactions slow compared to the universe expansion rate, so that the abundances of the various nuclides level off. These steady state values, called the the primordial abundances, are then the abundances of the various nuclides that persist until matter coalesces into stars some hundreds of millions of years later.

In standard ΛCDM cosmology, BBN is essentially parameter-free, as all of the contributing inputs– the baryon-to-photon ratio $\eta := \frac{n_B}{n_\gamma}$ (n_B, n_γ are the number densities of baryons and photons, respectively), the neutron lifetime, various nuclide binding energies, and the cross sections of the many nuclear reactions– can be be measured independently, and their experimental range of uncertainty affects the resulting abundances very little. It is therefore seen as one of the most compelling successes of Cosmology that the
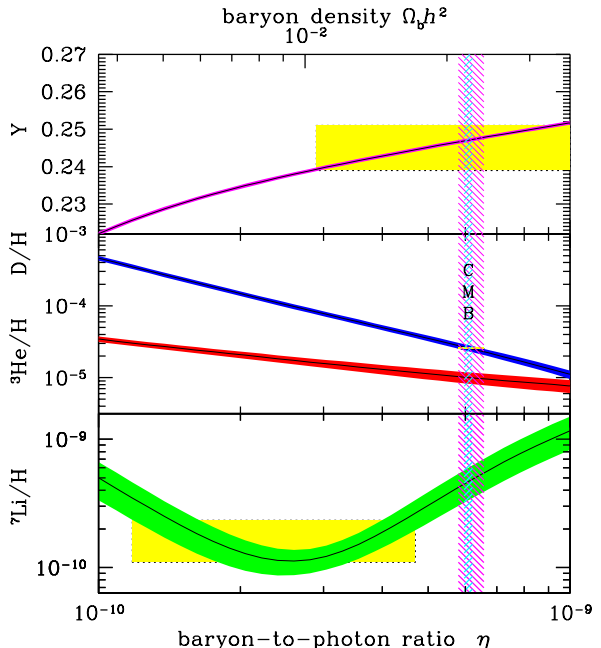

Figure 5: Predicted light element primordial abundances from standard BBN as a function of the baryon-to-photon ratio η. Colored thickenings of the black curves indicate the uncertainty in each prediction, whereas the yellow boxes indicate the regions of agreement between the predictions of each nuclide abundance and its measured value (no such region is generated for ^{3}He). The vertical blue shaded region represents the η range in agreement with CMB observations, and the thicker red region the range in which both ^{4}He and deuterium abundances are consistent with measurements. Image generated by the Particle Data Group [20].

predicted primordial abundances of deuterium and ^{4}He (the latter reported in terms of its mass fraction Y) agree exceedingly well with their measured values [20],

$$Y|_{\rm p} = 0.245 \pm 0.003 \qquad (12)$$

$$D/H|_{\rm p} = (25.47 \pm 0.25) \times 10^{-6}, \qquad (13)$$

given the η value (perhaps the parameter to which the abundances are most sensitive) measured via the CMB anisotropy by the *Planck* collaboration [1],

$$\eta \times 10^{10} =: \eta_{10} = 6.105 \pm 0.055. \qquad (14)$$

Beyond ^{4}He and deuterium, BBN also predicts nontrivial primordial abundances for ^{3}He and ^{7}Li. While there are challenges in measuring these abundances, measurements at least suggest the qualitative success of BBN in that they return orders of magnitude consistent with predictions. In the case of ^{3}He, inconsistencies between measurement sources together with open questions in stellar evolution

models make it difficult to establish a single measured value for the primordial ^{3}He abundance, so it cannot yet be used reliably as a Cosmological probe.

The situation of ^{7}Li is more problematic for BBN, as the theoretical prediction of ^{7}Li/H$|_p = (5.623 \pm 0.247) \times 10^{-10}$ [17] is some 3.5 times larger than the measured value of $(1.6 \pm 0.3) \times 10^{-10}$ [20]– this is known as the *lithium problem*. It's possible this discrepancy is due to challenges determining a measured value, in particular the unexplained large scatter in ^{7}Li abundances in stars with very low metallicities [Fe/H] < -3.0 which inhibits extrapolation to 0 metallicity (the primordial situation), but this is seen as unlikely because the stellar mechanisms for depleting ^{7}Li aren't thought to be nearly efficient enough to reduced the predicted primordial abundance down to the value measured within moderately metallic stars [20]. Further, the relevant nuclear reaction rates are experimentally well enough constrained that it is unlikely that the lithium problem will be resolved through nuclear physics [17]. New physics hypotheses proposed to resolve the lithium problem abound, but none have yet emerged as thoroughly convincing.

3 Computing Primordial Abundances in the Presence of SFDM

3.1 BBN ODEs and Methods

The primordial abundances depend crucially on the time evolution of the scale factor $a(t)$ of the homogeneous and isotropic universe, as the timing of the freeze out processes is determined by a comparison between the expansion rate $H(t)$ and the reaction rates. Since SFDM cosmology allows for ρ_ψ to dominate the total energy density during the $\rho_\psi \propto a^{-6}$ era, it can qualitatively change the evolution of $a(t)$ during nucleosynthesis, so we are led to ask how this alteration to the scale factor can adjust primordial abundance predictions. To answer this question, we modified a pre-existing BBN code, PArthENoPE (Public Algorithm Evaluating the Nucleosynthesis of Primordial Elements), built upon the foundation of earlier codes by Kawano [9] and Wagoner [22]. In the following, we follow the notation and treatment of the works published accompanying the PArthENoPE code [16], [7].

The system of ODEs determining the time evolution of BBN with SFDM is comprised of equations (6)-(8), where equation (7) will now only apply to the total energy density and total pressure

$$\rho = \rho_B + \rho_\gamma + \rho_e + \rho_\nu + \rho_\psi \qquad (15)$$
$$p = p_B + p_\gamma + p_e + p_\nu + p_\psi \qquad (16)$$

as there is exchange of energy between matter sources, together with conservation of baryon number, charge neutrality, and the collection of Boltzmann equations for each of the tracked nuclides. Denoting by n_B the baryon number density, $X_i := \frac{n_i}{n_B}$ and Z_i the relative abundance and proton number of the ith nuclide type, and $\phi_e := \frac{\mu_e}{T}$ with μ_e the (temperature-dependent) electron chemical potential, these three new equations are, respectively,

$$\frac{\dot{n}_B}{n_B} = -3H \qquad (17)$$

$$n_B \sum_j Z_j X_j = n_{e^-} - n_{e^+} = T^3 \hat{L}\left(\frac{m_e}{T}, \phi_e\right) \qquad (18)$$

$$\dot{X}_i = \sum_{j,k,l} N_i \left(\Gamma_{kl \to ij} \frac{X_l^{N_l} X_k^{N_k}}{N_l! N_k!} - i, j \leftrightarrow k, l\right). \qquad (19)$$

Here, the quantity $\Gamma_{kl \to ij}$ is the (temperature-dependent) rate, determinable from measured cross-sections, for the reaction yielding the ith and jth nuclides with the kth and lth nuclides as reactants. The positive integer N_i is the number of the ith nuclide produced in the reaction (similarly for N_j, N_k, and N_l, though the latter two are numbers consumed). Per the Fermi-Dirac distribution, the function $\hat{L}$ appearing in (18) describing the number density difference between electrons and positrons is

$$\hat{L}(\xi, \omega) = \frac{1}{\pi^2} \int_\xi^\infty \left(\frac{\zeta\sqrt{\zeta^2 - \xi^2}}{e^{\zeta - \omega} + 1} - \frac{\zeta\sqrt{\zeta^2 - \xi^2}}{e^{\zeta + \omega} + 1}\right) d\zeta.$$

The baryon energy density ρ_B and pressure p_B are computed via n_B, the relative abundances X_i, the nuclide binding energies, and the photon temperature T, while those of electrons, neutrinos, and photons are computed using their momentum space distribution functions appropriate to their being in thermodynamic equilibrium. Hence, if we model a network of reactions among N_{nuc} nuclides, the $5 + N_{\text{nuc}}$ equations in the above system have $5 + N_{\text{nuc}}$ unknowns: ψ, H, n_B, T, ϕ_e, and the relative abundances X_i.

We take initial conditions at $T = 10$ MeV, before the weak interaction has shut off, so that all relative abundances (most importantly those of neutrons and protons) are at their equilibrium values. The initial n_B is determined by the baryon-to-photon ratio η and the current CMB temperature. The initial H and ϕ_e are set by equations (8) and (18), respectively.
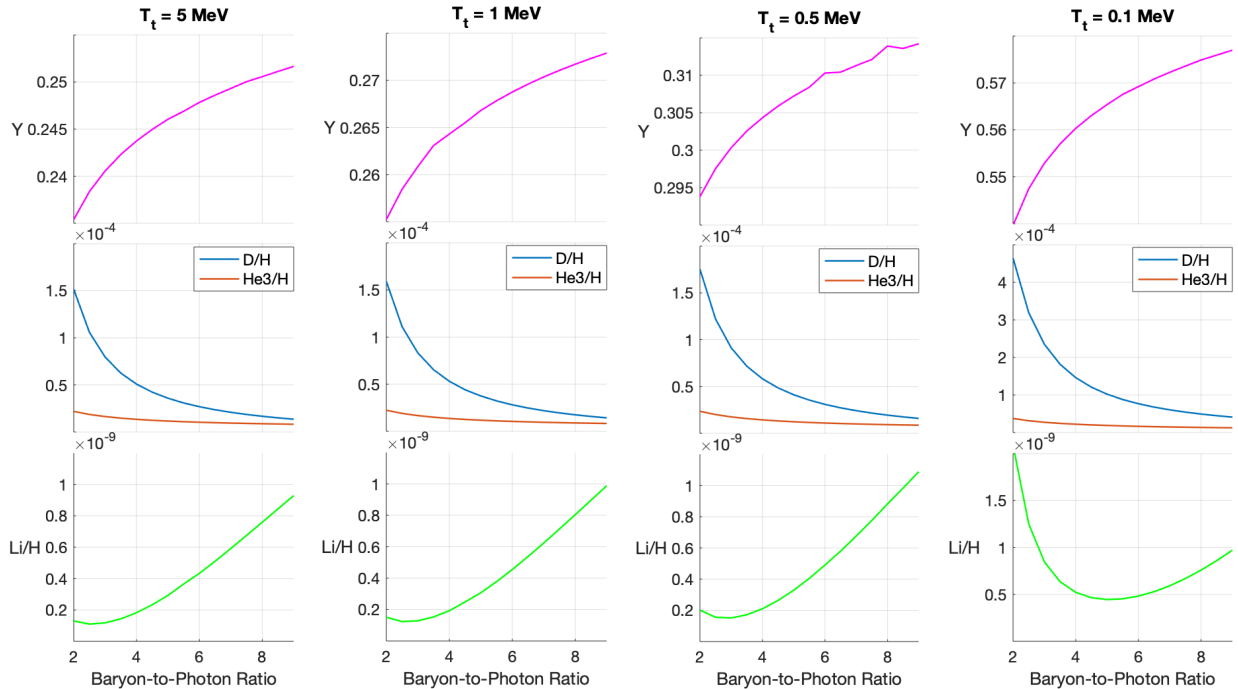
6

Figure 6: Predicted light element primordial abundances from BBN with SFDM for various values of the transition temperature T_t, plotted versus η_{10}. Notice that the scale of the y-axis in the top row (reporting the Helium-to-Hydrogen mass ration Y) changes from column to column, while the scales in the bottom two rows only change in the last column.

The initial values for ψ and $\dot{\psi}$ are constrained by the requirement that ρ_ψ evolves to the current observed dark matter density, measured by *Planck* to satisfy $\Omega_{\mathrm{dm}}h^2 = 0.1200 \pm 0.0012$ [1], but there remains a degree of freedom in the choice of initial $\psi, \dot{\psi}$ that amounts to choosing the temperature T_t at which the ρ_ψ-dominated era ends, i.e. at which $\rho_\psi = \rho_\gamma + \rho_e + \rho_\nu$. There is, in principle, the additional free parameter of the SFDM mass m, but we expect it to have very little effect on the abundances once the transition temperature T_t and the current-day ρ_ψ have been set, as these parameters largely determine the temperature dependence of ρ_ψ. It warrants mentioning that [2] also sought to evaluate the influence of SFDM on BBN, but it seems they arbitrarily constrained their range of T_t values such that ρ_ψ was always negligible during BBN.

We modified the PArthENoPE code, which solves a more numerically convenient recasting of the system of equations (7), (8), and (17)-(19) detailed in [16], to include the dynamics of a scalar field through equation (6) and its contribution of ρ_ψ, p_ψ to the energy density and pressure. Our quoted results will use a network of the $N_{\mathrm{nuc}} = 9$ lightest nuclides, related via some 40 nuclear reactions. See [19] for a detailed review of the nuclear reactions important to BBN and [17] for a discussion of subtle corrections to the simplest implementations of BBN.

3.2 Abundances Results

Our numerical results for the light element abundances in the presence of SFDM are presented above in Figure 6. The leftmost column, $T_t = 5$ MeV, is essentially the standard BBN scenario, as the SFDM energy density is effectively negligible compared to radiation by the time nucleosynthesis-relevant processes begin around $T \sim 1$ MeV (when the neutron-to-proton ratio n/p freezes out) in this case. As one decreases the transition temperature, SFDM becomes more and more important to the scale factor evolution during nucleosynthesis.

The most notable effect of SFDM's becoming more significant is an increase in the predicted abundances across the board, though this increase is slight for lithium, deuterium, and ^{3}He in the $T_t = 1$ MeV and $T_t = 0.5$ MeV cases. Worse than the fact that this pushes the Lithium prediction further from its measured value, however, even in these cases the perturbation to the energy density already pushes the ^{4}He mass fraction Y squarely out of concordance with the

measurements reported in equations (12) and (14).

In the $T_t = 0.1$ MeV case, SFDM has non-negligible energy density during the nucleosynthesis processes themselves (rather than just the n/p freeze out process), and this makes a somewhat dramatic difference in our results: now all of the predicted abundances are shifted up by an appreciable amount (less so only for ^{3}He). The ^{4}He mass fraction is now more than double the measured value, and the deuterium prediction is also well outside of the range compatible with equation (13). Of course, the lithium situation has only gotten worse.

4   Conclusion and Future Work

Generally speaking, we've found that the first-order adjustments due to extending the $\rho_\psi \propto a^{-6}$ era of SFDM Cosmology appear to do little to alleviate the lithium problem of BBN, and even slightly more dramatic adjustments seem starkly incompatible with observations. Indeed, allowing ρ_ψ to be nontrivial during nucleosynthesis primarily serves to increase the matter density and hence the Hubble parameter H by equation (8), which should heuristically have the effect that freeze outs occur earlier (at higher temperatures) while ρ_ψ is large. In particular, if $T_t \lesssim 1$ MeV this causes n/p to freeze out while the equilibrium value is larger; this increase in available neutrons for nucleosynthesis should increase the production of nuclides (especially ^{4}He, the primary neutron receptacle), tending to shift the predicted ^{7}Li abundance upward away from the measured value. By further pushing down T_t to $T_t \lesssim 0.1$ MeV, one allows the nontrivial ρ_ψ to influence the dynamics of the nucleosynthesis reactions themselves, but this both further increases n/p and increases the likelihood that the adjustment destroys the successful predictions of the deuterium and ^{4}He abundances. Our numerical results seem to reinforce these heuristic objections.

These results and heuristic arguments are not yet fatal to a SFDM resolution to the lithium problem, however. The author has (quite) recently realized that the PArthENoPE code has the electron, neutrino, and photon energy densities hard-coded as functions of temperature based upon their distribution function dynamics in a radiation-dominated background (this can reasonably be done in standard BBN because the Baryon energy density is negligible compared to these radiation sources, so their dynamics may be solved independently), so that the neutrino and photon energy densities used were not quite correct for the SFDM scenario. There is good theoretical reason to expect that the error in these quantities is rather low after electron-positron annihilation completes (simply shifting the effective number of neutrino species N_{eff} from 3.046 closer to 3) by around $T \sim 0.1$ MeV, so during nucleosynthesis itself, but it may be important during and before this annihilation, including when the ratio n/p freezes out.

Equally important to recognize is that, irrespective of the magnitude of the above correction, the results presented here do not indicate that SFDM is in tension with abundance measurements– it only indicates that the transition temperature T_t must satisfy $T_t \gtrsim 5$ MeV. So long as this is the case, the SFDM does not change predictions from standard BBN.

Finally, we comment on the case of a complex scalar field. As noted previously, a complex field is equivalent to two independent real scalar fields. Though these fields will each have their own transition temperature at which they dominate radiation, the total energy density (and hence nucleosynthesis results) will be effectively the same as in the case of a real scalar field with transition temperature the smaller of these two. That being said, if it is required that the two fields oscillate out of phase at late times so that they can condense directly into the static ground states recognized as the only known long-time stable configurations of low-field SFDM [14] [3], then the earlier of these transition temperatures is forced to occur right at $H \sim m$. Noting that the results of section 3.2 seem to require $T_t \gtrsim 5$ MeV, this yields a tentative lower bound $m \gtrsim 10^{-20}$ eV.

Future work should certainly include evaluating the impact of correcting the photon and neutrino energy densities. Intimately related investigations the author has begun pursuing are the implications of the $\rho_\psi \propto a^{-6}$ era for other hallmark features of Cosmology, such as the matter power spectrum and CMB anisotropy.

Also in the vein of dark matter, the author is interested in determining the viability of a massive vector field theory of fuzzy dark matter, which must satisfy a wave equation qualitatively similar to the Klein-Gordon equation of SFDM, so one might expect similar behavior. Current limits on the photon mass [20] do not seem to unequivocally rule out the possibility that such a vector field might be that of electromagnetism, though it need not be that of electromagnetism to provide a dark matter candidate. Preliminary evaluation of low-field, static, spherically symmetric solutions (analogous to that class of SFDM solutions often put forward as galaxy models) to the equations of motion of a massive vector field, however, seems to indicate some qualitative differences from the SFDM case that may not be reconcilable with observations of galaxies.

A last, somewhat far afield topic of research the author is interested in and has worked on briefly is the Cosmic Censorship Conjecture, particularly in spherical symmetry. This work was inspired by the group's publication on the topic of flatly foliated relativity [4] last year.

References

[1] N Aghanim, Yashar Akrami, M Ashdown, J Aumont, C Baccigalupi, M Ballardini, AJ Banday, RB Barreiro, N Bartolo, S Basak, et al. Planck 2018 results. vi. cosmological parameters. *arXiv preprint arXiv:1807.06209*, 2018.

[2] A Arbey and J-F Coupechoux. Cosmological scalar fields and big-bang nucleosynthesis. *Journal of Cosmology and Astroparticle Physics*, 2019(11):038, 2019.

[3] Jayashree Balakrishna, Edward Seidel, and Wai-Mo Suen. Dynamical evolution of boson stars. ii. excited states and self-interacting fields. *Physical Review D*, 58(10):104004, 1998.

[4] Hubert Bray, Benjamin Hamm, Sven Hirsch, James Wheeler, and Yiyue Zhang. Flatly foliated relativity. *arXiv preprint arXiv:1911.00967*, 2019.

[5] Hubert L Bray. On dark matter, spiral galaxies, and the axioms of general relativity. *Geometric analysis, mathematical relativity, and nonlinear partial differential equations*, 599:1–64, 2010.

[6] Douglas Clowe, Maruša Bradač, Anthony H Gonzalez, Maxim Markevitch, Scott W Randall, Christine Jones, and Dennis Zaritsky. A direct empirical proof of the existence of dark matter. *The Astrophysical Journal Letters*, 648(2):L109, 2006.

[7] R Consiglio, PF de Salas, Giuseppe Mangano, Gennaro Miele, S Pastor, and O Pisanti. Parthenope reloaded. *Computer Physics Communications*, 233:237–242, 2018.

[8] Lam Hui, Jeremiah P Ostriker, Scott Tremaine, and Edward Witten. Ultralight scalars as cosmological dark matter. *Physical Review D*, 95(4):043541, 2017.

[9] Lawrence Kawano. Let's go: Early universe 2. primordial nucleosynthesis the computer way. 1992.

[10] William Thomson Baron Kelvin. *Baltimore lectures on molecular dynamics and the wave theory of light*. CJ Clay and Sons, 1904.

[11] Stacy Y Kim, Annika HG Peter, and Jonathan R Hargis. there is no missing satellites problem. *arXiv preprint arXiv:1711.06267*, 2017.

[12] Federico Lelli, Stacy S McGaugh, and James M Schombert. Sparc: mass models for 175 disk galaxies with spitzer photometry and accurate rotation curves. *The Astronomical Journal*, 152(6):157, 2016.

[13] David Lovelock. The four-dimensionality of space and the einstein tensor. *Journal of Mathematical Physics*, 13(6):874–876, 1972.

[14] Jeremy Louis Marzuola, SG Raynor, and Gideon Simpson. Nonlinear bound states in a schrodinger–poisson system with external potential. *SIAM Journal on Applied Dynamical Systems*, 16(1):226–251, 2017.

[15] Jeremiah P Ostriker, Ena Choi, Anthony Chow, and Kundan Guha. Mind the gap: Is the too big to fail problem resolved? *The Astrophysical Journal*, 885(1):97, 2019.

[16] O Pisanti, A Cirillo, Salvatore Esposito, F Iocco, Giuseppe Mangano, Gennaro Miele, and PD Serpico. Parthenope: Public algorithm evaluating the nucleosynthesis of primordial elements. *Computer Physics Communications*, 178(12):956–971, 2008.

[17] Cyril Pitrou, Alain Coc, Jean-Philippe Uzan, and Elisabeth Vangioni. Precision big bang nucleosynthesis with improved helium-4 predictions. *Physics Reports*, 754:1–66, 2018.

[18] VA Rubakov. Cosmology and dark matter. *arXiv preprint arXiv:1912.04727*, 2019.

[19] Pasquale Dario Serpico, S Esposito, F Iocco, G Mangano, G Miele, and O Pisanti. Nuclear reaction network for primordial nucleosynthesis: a detailed analysis of rates, uncertainties and light nuclei yields. *Journal of Cosmology and Astroparticle Physics*, 2004(12):010, 2004.

[20] Masaharu Tanabashi, K Hagiwara, K Hikasa, K Nakamura, Y Sumino, F Takahashi, J Tanaka, K Agashe, G Aielli, C Amsler, et al. Review of particle physics. *Physical Review D*, 98(3):030001, 2018.

[21] Luca Visinelli and Sunny Vagnozzi. Cosmological window onto the string axiverse and the supersymmetry breaking scale. *Physical Review D*, 99(6):063517, 2019.

[22] Robert V Wagoner. Big-bang nucleosynthesis revisited. *The Astrophysical Journal*, 179:343–360, 1973.